Chapter – 1

Literature survey and theoretical aspects of nonlinear optics, crystal growth and lattice imperfections

Abstract

The extensive survey of the importance of nonlinear optical single crystals in view of their photonic applications in Information & Technology for high density data storage, processing and transmission has been given. The historical importance of single crystals and their growth has been carried out. The fundamentals of the second harmonic generation and phase-matching have been discussed. Theoretical aspects of nucleation and crystal growth have been provided and the single crystal growth methods have been categorized. A discussion about the imperfections/ defects in single crystals has been carried out.

1.1 LITERATURE SURVEY

Due to high-speed and ease of production of photons (light), the area of photonics has become an active field of research in view of the modern society's demand for improved telecommunications, data storage, retrieving, processing and transmission. The design of devices that utilize photons instead of electrons for the transmission of information has created a need for new materials with unique nonlinear optical (NLO) materials (Williams, 1984). The nonlinear optics is the field which includes all phenomena in which optical parameters of materials are changed with the interaction of intense coherent source of light. The NLO phenomena have lead to the enhancement in understanding of light-matter interactions. The search for new molecular materials with NLO properties is currently the subject of considerable importance investigations due to their potential applications in photonic devices (Prasad & Williams, 1991). The invention of laser has created a revolution for research and development in the area of photonics and the investigations on NLO properties enhanced and widened the horizon of application of lasers. The drawback of most of the laser materials is their inability to generate the radiation in a wide spectral region, such as, for some applications the appropriate laser materials exist but due to thermal properties of source materials the emitted power is restricted. The nonlinear optics makes it possible to transfer the energy from wavelength to another and hence provide a solution for the radiation sources in the spectra range of radiation (Hannes *et al.*, 2010).

The history of nonlinear optics began early in 1875 with the observation of electric field induced change in the refractive index of CS_2 by Kerr (Kerr, 1875). In 1893, Pockel made similar kind of observations in quartz crystals (Pockels, 1893). However, the full realization of these theories could be realized with the discovery of laser having the intense beams (electric field), in 1960. Throughout the 1960's, Bloembergen and coworkers contributed significantly to the field of nonlinear optics (Bloembergen, 1965). In early 1970's, Davydov and co-workers (Davydov *et al.*, 1970) have demonstrated the strong second-order NLO effects in donor-acceptor substituted aromatic compounds. The finding of third order NLO effects in polydiacetylenes in 1976 by Sauteret and coworkers and the advent of optical fiber in

telecommunication in late 1970's given a boost up and broadened the horizon of research for NLO properties of organic materials (Sauteret *et al.*, 1976; Rustagi & Ducuing, 1974). The organic, polymeric and composite materials have emerged with interesting NLO properties (Chemla & Zyss, 1987; Flytzanis, 1986; Hann, 1989; Orenstein, 1987; Williams, 1983; Marder, 1991). Today, the research on NLO materials has been extended as interdisciplinary frontier of science and technology and assimilated with the disciplines of Chemistry, Physics, Optical Engineering and Materials science because of the applicability of NLO materials to many braches of information and image processing technologies.

The NLO single crystals therefore can be employed to generate the sources of different wavelengths for which the lasers are not available. The output radiation beam from a nonlinear optical device has the similar properties as those of a laser source, hence can be directly employed as laser source. For certain applications it is required to have highly powerful laser radiation (such as inertial confinement fusion research) (De Yoreo *et al.*, 2002). However, instead of attempting to scale up the laser itself it is simpler to amplify a well performing laser in a second stage. Thus the overall process is split into two steps where the generator will focus only on the generation of high quality signal, while the amplifier specifies in boosting the signal without adding too much noise. The nonlinear optical crystals are suggested to employ to amplify the coherent radiation. The invention of holography and nonlinear optics in the nonlinear dielectric materials has revolutionized the photonics for advanced technology of information (Gabor, 1948; Franken *et al.*, 1961; Armstrong *et al.*, 1962; Bloembergen, 1965).

The crystals are the most stable state of matter and admired the mankind, right from the pre-historic era of human civilization, '***Lord Rama offered an ornament made with diamonds to his most faithful and beloved warrior, Hanuman, on the occasion of great victory over Ravana***'. These have acquired an auspicious place for the spiritual and scientific development of human life. Mother Earth has abundance wealth of naturally crystallized materials like, quartz, diamond, ruby crystals, *etc.*, they are not only aesthetically pleasing but also of great importance to industry and economy growth. The art of crystallization extends far back in the past and antedates

considerably the written history of man. The crystallization of salt from sea water by evaporation was practiced at many places in the prehistoric time and has been considered as one of the oldest technical methods of transforming materials. The alchemist Geber, whose papers are dated in the 12th or 13th century (*cf.* Darmstaedter, 1922), described the preparation and purification of various materials by recrystallization as well as by sublimation and distillation. In the middle of the 16th century, Birriguccio (1540) recorded the leeching and recrystallization of saltpeter and the Saxonion scientist Agricola (1556) in his famous extensive work '*De re Metallica*' gave instructions on how to produce various salts, alums and vitrols by using strings for seeding [Feigelson, 2004]. In the following century, the word '*crystal*' came into use as modern name; originally, Homer had used the expression '*crystallos*' for ice crystals.

The modern scientific development of crystallography started in 17th century. In 18th century, Westfeld (1767), Bergman (1773), Haüy (1782) given the idea of smallest possible unit a '*molecule integrante*', by repetition of which whole crystal is built up and in 19th century Weiss (1804) considered the crystal to be as anisotropic continua; he derived the crystal system (1815) and discovered the law of rational intercepts (1816) and zone law (1820) [Feigelson, 2004]. Miller (1839) and Bravais (1849) have proposed the idea of Miller's indices and lattice types. Laue, Friedrich, Knipping (1912) and Bragg (1913) gave the X-ray diffraction law and crystal structure determination. Our quest for knowledge and technological advancement has made us to grow synthetic crystals as an alternative to the scarcely available natural crystals. The ideal crystal is defined as the infinite lattice of atoms arranged in particular pattern, which repeat in all three dimensions with repeated distances (lattice spacings), with all physical and electrical properties anisotropic in nature (Dryburgh, 1986). The real single crystals are finite in size but consist long-range order and also defects. The orders and defects result in the crystals with unique properties (Brandle, 1979; Brice, 1986).

Single crystal technology is the mother technology of almost all the recent technologies of the modern science. In the modern world, the large-scale use of these crystals has been brought about mainly by the demands of solid state physics of

materials for research and developments. A variety of crystals are needed to meet some very important gaps the conventional production engineering. Several kinds of single crystals find application for the development of technologies such as: laser, semiconductor, high and low energy particle physics, nuclear fusion, medical diagnostic, display, thermal imaging, *etc.* (Bailey, 1991; Nalwa & Miyata, 1996). To satisfy the need of science, technology and ornamental purposes, the artificial crystals are being produced. The ability to grow high quality crystals has become an essential criterion for the competitiveness of nations.

In the recent decade, NLO crystals have shown a promising role in photonics for high density optical data storage, quantum storage of photonic entanglement, cascaded photon-pair generation, acousto-optic interaction phenomenon applications (Lee *et al.*, 2000; Christoph *et al.*, 2011; Hannes *et al.*, 2010; Mark Haw, 2003; Lounis, & Moerner, 2000; McPherson *et al.*, 2002). The NLO crystal research is strongly motivated and based on inorganic materials such as $LiNbO_3$, GaAs, InP, *etc.*, with good mechanical stability and sufficiently large NLO coefficients. A series of inorganic NLO crystals have been investigated and reviewed (Nikogosyan, 2005). Lithium niobate ($LiNbO_3$) is an excellent NLO material with various pronounced physical properties. It has been particularly fruitful in the optical regime, where many effects have been found in $LiNbO_3$ and devices introduced using it as a host. Its photorefraction property has been considerably important for applications such as holographic volume data storage, optical image and signal processing, phase conjugation, real time interferometry, beam deflection and novelty filters (Gunter & Huignard, 1988, 1989). The structure and density of intrinsic (non-stoichiometric) defects substantially influence the optical properties, including the photorefractive effects (Anghert *et al.*, 1972; Furukawa, 1992; Malovichko *et al.*, 1993; Arizmendi *et al.*, 1991). $LiNbO_3$ have been efficiently used for the optical parametric amplification applications (Giordmaine & Miller, 1965; Kingston, 1962; Malcolm & Majid, 1999; Ebrahimzadeh & Dunn, 2000). Waveguides, optical dispersion, acoustic resonators, transducers, acousto-optic, ultrasonic waves (100 MHz-10 GHz), surface acoustic waves (SAW), *etc.* applications of lithium niobate have been successfully performed (Wong, 2002). Due to the anisotropic nature of single crystals, the properties strongly

depend on the specimen grain boundaries, dislocations, impurities and inclusions, also influenced by the electric/magnetic domain boundaries in ferroelectric/ferromagnetic media, $LiNbO_3$ is of ferroelectric class.

However, the organic materials exhibited the larger NLO efficiencies due to their purely electronic response, and therefore promise to meet future requirements for ultrahigh bandwidth photonic devices (Eaton, 1991; Zyss, 1994; Günter, 2000; Dalton, 2002, Jazbinsek, 2008; Williams *et al.*, 1984; Williams *et al.*, 1983; Marder, *et al.*, 1989). Due to the immense important of NLO crystals, it is useful to synthesis new NLO materials, grow in single crystals form and study their structural, physical, thermal and optical properties. The active π-bonds in organic materials make them flexible to engineer their structure, which drag the attention of researchers to a great extent. Therefor the high NLO effect of organic materials could have been combined with the high mechanical and thermal stability of inorganic materials to form the semi-organic NLO materials. In the recent decades extensive research has been carried out on such materials. The semiorganic materials exhibited the large nonlinearity, high resistance to laser damage, low angular sensitivity and good mechanical hardness (Marcy *et al.*, 1992; Velsko, 1990; Xing *et al.*, 1987). The complexes of urea and urea analogs, such as tris(thiourea)zinc sulphate (ZTS), bis(thiourea)zinc chloride (ZTC), bis(thiourea)cadmium chloride (BTCC), *etc.* have been explored for NLO applications (Newman *et al.*, 1990). A series of thiocyanates bimetallic complexes found to exhibit the efficient second harmonic generation at short wavelengths (Nakamoto, 1986).

In parallel to the invention of new NLO materials it is also equally important to improve the structural and physical properties of crystals for the tailor made applications, by using suitable dopants and addition of functional groups to the available materials. Growth of NLO single crystals of bulk size of good quality using the suitable technique is of great importance from the device application point of view. As defects affect the properties of crystals and hence the efficiency of device, therefore, it becomes of stringent importance to investigate the grown crystals for structural defects (point defects, dislocations and their agglomerates, structural grain boundaries), which arise during their growth or post growth treatments.

1.2 THEORETICAL ASPECTS OF NONLINEAR OPTICS

1.2.1 Nonlinear optics

In the pre-laser era the optical properties of the materials were considered to be linear independent of the intensity of radiation. The basis for this conclusion for this conclusion is that the filed strengths of the conventional light sources before the advent of lasers were much smaller than the field strengths of atomic and inter-atomic fields. The latter are of the order of 10^7 - 10^{10} V/cm whereas the former would not exceed 10^3 V/cm. The light sources with such a low intensity are not able to affect the atomic fields to the extent of changing the optical parameters. The laser radiation with high degree of coherence made it possible to attain the high spatial concentration of light power. It is now possible to generate 1 MW pulses, lasting a few tenths of nanosecond, using moderately powerful lasers. The energy current density in a beam of cross-section 1 mm^2 of such a laser is $J_E \approx 10^6$ MW/m^2, which corresponds to peak electric field strength $E \approx 3 \times 10^7$ V/m, due to coherence, the beam can be focused to an area $A \approx \lambda^2$. If the laser wavelength is assumed to be 1 μm, then $A = 10^{-12}$ m^2 and hence $J_E \approx 10^{18}$ MW/m^2 giving $E \approx 3 \times 10^{10}$ V/m, which is within the range of atomic fields. Under such high fields, the relationship between the electric polarization *P* and the field strength E ceases to be linear and some interesting nonlinear effects come to the fore.

1.2.2 Harmonic generation

Just after the invention of lasers, the nonlinear properties in the optical medium have been strikingly demonstrated by the harmonic generation of light observed for the first time by *Franken* and his coworkers in 1961 (Franken *et al.*, 1961). They have observed ultraviolet light (λ = 3472 Å) at twice the frequency of a ruby laser (λ = 6493 Å), when the light was made to traverse a quartz crystal. This experiment attracted the widespread attention and marked the beginning of the experimental and theoretical investigation of nonlinear optical properties. The theoretical aspect of nonlinear optical behavior of the dielectric medium is illustrated as follows.

When a dielectric medium is placed in an electric field it gets polarized. Each molecule acts as a dipole, with a dipole moment P_i which results in the dipole moment vector per unit volume P, given by $P = \sum_i P_i$, here summation is over the dipoles per unit volume. The orientation effect of the external field on the molecular dipoles depends both on the properties of the medium and strength of the field. Hence, P can be expressed as a function of field E;

$$P = \varepsilon_o \chi E \tag{1.1}$$

here, χ is called the *polarizability* or *dielectric susceptibility* of the medium.

The above relation is valid for the field strengths of conventional sources. The χ value is a constant only in the sense of being independent of E; its magnitude is function of frequency. For the intense laser source this relation does not hold good and has been generalized to

$$P = \varepsilon_o (\chi^{(1)} E + \chi^{(2)} E^2 + \chi^{(3)} E^3 + ...) \tag{1.2}$$

here, $\chi^{(1)}$ is same as χ in (1.1) and the coefficients $\chi^{(2)}$, $\chi^{(3)}$, … define the degree of nonlinearity and are known as nonlinear susceptibilities. If the field is low, as it is in the case of ordinary light sources, only first term of (1.2) is to be retained. Higher the value of the electric field, more significant becomes the higher order terms. It may be noted that optical characteristics of medium, such as dielectric permittivity, refractive index, *etc.*, which depend upon susceptibility, also become the functions of field strength E, if it is sufficiently high. The medium which follows the nonlinear relation of polarization (1.2) is called a *nonlinear optical medium*.

If the incident field is of sinusoidal nature of the form

$$E = E_o \cos \omega t \tag{1.3}$$

Then we have P of the form

$$P = \varepsilon_o \chi^{(1)} E_o \cos \omega t + \varepsilon_o \chi^{(2)} E_o^2 \cos^2 \omega t + \varepsilon_o \chi^{(3)} E_o^3 \cos^3 \omega t + ...$$

Using the trigonometric relations we get the resultant equation as follows

$$P = \frac{1}{2}\varepsilon_o \chi^{(2)} E_o^2 + \varepsilon_o \left(\chi^{(1)} + \frac{3}{4}\chi^{(3)} E_o^2 \right) E_o \cos \omega t + \frac{1}{2}\varepsilon_o \chi^{(2)} E_o^2 \cos 2\omega t + \frac{1}{4}\varepsilon_o \chi^{(3)} E_o^3 \cos 3\omega t + ... \tag{1.4}$$

The first term of (1.4) is a constant term, it gives rise to a dc field across the medium, the effect of which is of comparatively less importance. The second follows

the external polarization and is called the *first* or *fundamental harmonic of polarization*; the third oscillates at a frequency 2ω and is called the *second harmonic of polarization*, the fourth is called the *third harmonic of polarization*, and so on.

1.2.3 Second harmonic generation

In second harmonic generation (SHG), the light frequency is doubled, essentially converting two photons of the original beam of energy E into a single photon of energy $2E$ as it interacts with noncentrosymmetric media. The theoretical treatment of harmonic generation is given in the previous section. In this section we will discuss more about the SHG. The second order NLO materials are used in optical switching (modulation), frequency conversion, and electro-optic (EO) applications. All of these applications rely on the manifestation of the molecular hyperpolarizability of the materials. In most crystalline materials, the nonlinear polarizability $\chi^{(2)}$ depends on the direction of propagation, polarization of the electric field and the orientation of the optic axis of the crystal. Since in such crystalline materials the vectors P and E are not necessarily parallel, the coefficients χ must be treated as tensors. The second order polarization may therefore be represented by the relation

$$P_i^{(2)} = \varepsilon_o \sum_{j,k} \chi_{ijk}^{(2)} E_j E_k \tag{1.5}$$

where *i, j, k* represent the coordinates *x, y, z*,. Most of the coefficients χ_{ijk}, however, are usually zero and we have to deal only with one or two components.

It is important to mention here that the second harmonic generation, represented by equation (1.5), occurs only in certain types of crystals. Consider, for example, a crystal that is isotropic. In this case χ_{ijk} is independent of direction and, hence, is a constant. If we now reverse, the direction of axis ($x \rightarrow -x$, $y \rightarrow -y$, $z \rightarrow -z$) leaving the electric field and dipole moment unchanged in the direction, the sign of these two must change. Therefore, $-P_i^{(2)} = \varepsilon_o \sum_{j,k} \chi_{ijk}^{(2)} (-E_j)(-E_k) = +P_i^{(2)}$; which means $P_i^{(2)} = 0$ and, hence, $\chi_{ijk}^{(2)} = 0$. Second harmonic generation, therefore, cannot occur in the isotropic medium such as liquids or gases nor in centro-symmteric crystals (i.e. crystals symmetric about a point). Only crystals that lack in inversion symmetry exhibit SHG. Therefore, for non-centrosymmetric crystals we can write the

polarization relation as $P = \varepsilon_o \chi^{(1)} E + \varepsilon_o \chi^{(2)} E^2$, and the crystal is said to possess the second order linearity.

The efficiency of generation of harmonics depends not only on the intensity of the exciting radiation, but also on its direction of propagation in crystals. If we consider a slab of crystal of length *L*, then the second harmonic radiation produced by the slab at the exit slab is given by, $E_{(L)}^{(2)} \alpha \sin\left(\frac{2k_1 - k_2}{2}\right) L \Big/ \left(\frac{2k_1 - k_2}{2}\right)$, where k_1 and k_2 are the propagation vectors ($k = 2\pi n/\lambda$, n is the refractive index at the wavelength λ) of fundamental and second harmonic radiations, respectively. In general $k_1 \neq k_2$ because of the wavelength dispersion of materials. The SHG signal will have the maximum value when $\frac{(2k_1 - k_2)L}{2} = \frac{\pi}{2}$, which results in the solution $L = \frac{\lambda}{4(n^{\omega} - n^{2\omega})}$, where n^{ω} and $n^{2\omega}$ are the refractive indices at ω and 2ω respectively. This value of L is called the *coherence length* for the second harmonic radiation (termed as L_c) and increasing its value beyond L_c, does not result into any increase in $E^{(2)}$. The intensity if given by the expression,

$$I = (E_{(L)}^{(2)})^2 = \sin^2\left(\frac{2k_1 - k_2}{2}\right) L \Big/ \left(\frac{2k_1 - k_2}{2}\right)^2 \qquad (1.6)$$

The variation of I and the peak of this plot is very sharp for the condition $k_2 = k_1$, which must be satisfied in case of efficient frequency doubling; the graph is shown in Fig. 1.1(b). This condition is known as the *phase-matching* criterion, which leads to the relation of the refraction indices of the fundamental wave and second harmonic waves as $n^{2\omega} = n^{\omega}$. It is rather difficult to fulfill this criterion because most of the materials show some sort of dispersion in refractive index [Fig. 1.1(a)]. In general Δk ($= k_1 - k_2$) is nonzero, the intensity '*I*' oscillates in a sine-square. If however, Δk approaches zero, the limit has to be calculated $\lim_{\Delta k \to 0} \frac{\sin(\Delta k L/2)}{\Delta k/2} = L$, In this case, the second-harmonic intensity increases quadratically with L – at least as long as we are in the limit of low second-harmonic intensities where the fundamental intensity is unchanged (Armstrong *et al.*, 1962; Tunyagi, 2004).

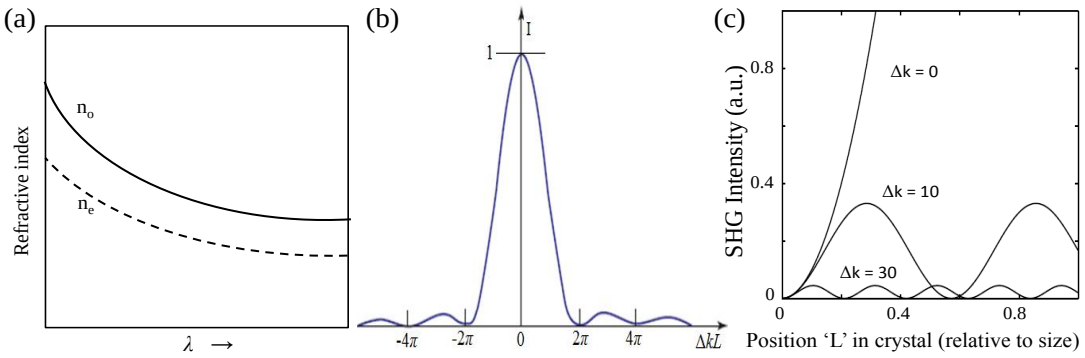

Fig. 1.1: *(a) wavelength dispersion of refractive index and its dependency on the polarization light, (b) I vs. ΔkL plot with maxima at $k_2 = k_1$ (Bloembergen, 1965), and (c) the second-harmonic intensities as a function of the position in the NLO material for different Δk values, in non-phase-matched case, with the second-harmonic power oscillating between zero and a small value (Manfred Wöhlecke et al., 2005)*

The spatial variation of second-harmonic intensities for the different characteristic values of Δ*k* is shown in Fig. 1.1(c). For a noncentrosymmetric crystal suitable for the efficient device application, the physical properties such as high effective nonlinear coefficient, good optical quality, wide transparency, good mechanical and chemical stability, large birefringence, low optical absorption, easy fabrication process, *etc.* are also essential.

The non-linear effect makes the conversion efficiency proportional to the *square* of the input power until the material saturates. Thus, high peak power is needed to achieve the best performance. This explains why pulsed lasers can be easily frequency doubled using external non-linear crystals but intracavity frequency doubling is much more effective for continuous wave (CW) lasers. Second harmonic generation should be viewed as a two-step process.

The second harmonic conversion efficiency 'η' of a NLO crystal is given by the expression

$$\eta = \frac{P^{2\omega}}{P^{\omega}} = 2\left(\frac{\mu_o}{\varepsilon_o}\right)^{3/2} \frac{\omega^2 d^2 l^2 \sin^2(\Delta k l/2)}{n^3 (\Delta k l/2)^2} \frac{P^{\omega}}{A} \tag{1.7}$$

where, μ_o, ε_o, n, ω, l, A and d are respectively the permeability of free space, permittivity of free space, index of refraction, angular frequency of fundamental wave, length of crystal, cross area of beam, respectively

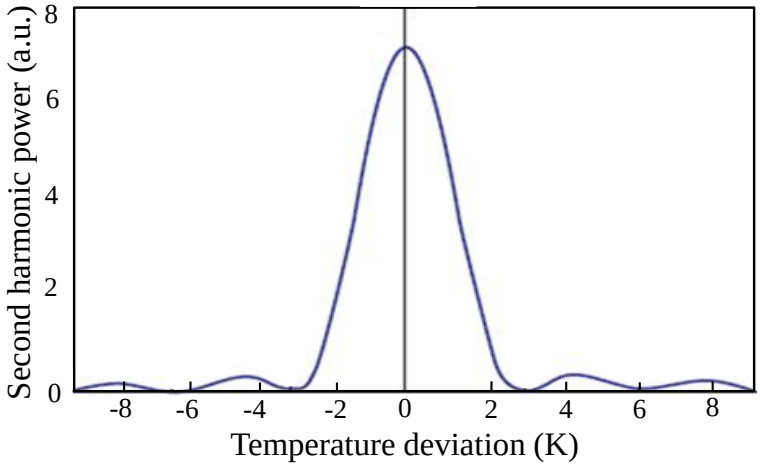

Fig. 1.2: *Second-harmonic power versus temperature deviation from the optimum point, assuming a homogeneous temperature distribution in the crystal and the constant pump intensity (low conversion efficiency) (http://www.rp-photonics.com/phase_matching.html)*

and effective nonlinear coefficient. The value of η also depends on the phase mismatch of the interacting waves, power of incident laser beam, refractive index of crystal, direction of incident beam with respect to optical axis.

When the crystal temperature is varied around the optimum point, the phase mismatch and thus the conversion efficiency also vary, as shown in Fig. 1.2. The temperature range in which the high conversion efficiency is obtained is inversely proportional to the crystal length. It also depends on the temperature dependence of the refractive indices involved. The expression for the temperature sensitivity of the crystal with respect to the second harmonic generation is,

$$\Delta T = \frac{0.44\lambda_1}{ld(n_o^{2\omega} - n_o^{\omega})/dT} \tag{1.8}$$

where ΔT is the full width at half maximum (FWHM) of the temperature range over which second harmonic generation is possible in a particular crystal. These temperature changes in doubling crystal may be the result of ambient temperature variations, or they may be caused by absorption losses in the crystal.

Absorption in crystal during the conversion efficiency measurements leads to thermal gradients as well as thermally induced stresses. Thus the associated refractive index variation severely restricts the crystal volume over which phase matching can be achieved. Also, in high power continuous laser experiments, generation of heat

inside the medium due to absorption is the main problem. A self-induced thermal distribution in the nonlinear medium can be caused by absorption of the fundamental or harmonic beams or multiphoton absorption processes.

1.2.4 Phase matching

For efficient frequency conversion, in nonlinear processes, such as harmonic generation, sum and difference frequency generation *etc*., phase matching is essential. This means ensuring that a proper phase relationship between the interacting waves is maintained along the propagation direction. Only if that condition is fulfilled, amplitude contributions from different locations to the product wave are all in phase at the end of the nonlinear crystal. In other words, *phase mismatch* caused by the dispersion of the medium should be close to zero in order to obtain an effective nonlinear interaction. Phase-matching is a method to compensate the phase difference between the interacting waves and thus optimize the conversion efficiency in the nonlinear process. The phase matching process describes when energy is transferred from fundamental frequency wave to the wave of harmonics of the fundamental frequency wave, traveling at the same velocity. The complex amplitude contributions from different parts of the nonlinear crystal for the harmonic wave add up constructively only when phase matching is achieved, and high power conversion efficiency is achieved. Otherwise, the direction of energy transfer changes periodically (possibly thousands of times during the passage through the crystal) according to the change in the phase relation between the interacting waves. The energy then oscillates between the waves rather than being transferred in a constant direction as illustrated in Fig. 1.1(c).

1.2.5 Phase matching techniques

For efficient energy transfer, the fundamental as well as its harmonics (however, we restrict ourselves to second harmonic as the thesis work is concerned with this) must remain in phase. But for real materials, the refractive indices n_1 and n_2 of the fundamental and second harmonic are generally not equal due to optical dispersion and the E/M wave will lag behind the polarization wave. Over very short distances, this will be slight and the waves will be substantially in phase. Output power will flow back and forth between the polarization wave and the E/M wave

along the length of interaction based on this phase mismatch. One half of the period is termed as the '*coherence length*' (not to be confused with the coherence length of a laser to which it is not related). The coherence length may be defined as the length of the medium in which the phase of pump and the sum of idler and signal frequencies are 180 degrees from each other. At each coherence length, the crystal axes are flipped which allows the energy to continue to positively flow from the pump to the signal and idler frequencies. However, this coherence length is typically very small resulting in insignificant amounts of second harmonic power - no more than is produced after one coherence length no matter how long the crystal is. The phase matching condition can be achieved by different ways: birefringent phase matching, temperature tuning, quasi-phase matching or periodic poling *etc.*

1.2.5.1 Birefringence phase matching

The usual technique for achieving phase matching in nonlinear crystals is birefringent phase matching, where one exploits birefringence of material (i.e., the refractive index depends on the polarization and direction of the light that passes through.), to cancel the phase mismatch. This technique comes in many variations. The restriction of limited coherence length is removed and taken the advantage of the natural birefringence for achieving phase matching in nonlinear crystals. Birefringence results in slightly different index of refraction values depending on the direction of polarization of the wave in the crystal due to anisotropy [Fig. 1.1(a)]. If it was possible to arrange the orientation of the crystal such that the incident (fundamental) and output (harmonic) beams propagated in just the proper directions such that n_1 would be exactly equal to n_2, the coherence length, and thus the power output, could be greatly increased. It turns out that materials like KDP, KTP, LBO, BBO, and $LiNbO_3$ have suitable dispersion characteristics for phase matching to be accomplished and high enough non-linear coefficient, damage thresholds, and other properties to make them useful for harmonic generation as well as other non-linear optical processes like optical mixing, OPOs (Optical Parametric Oscillators), OPAs (Optical Parametric Amplifiers), *etc.*

This type of birefringence phase matching relates to the polarization directions of the input and output beams and has been categorized as follows:

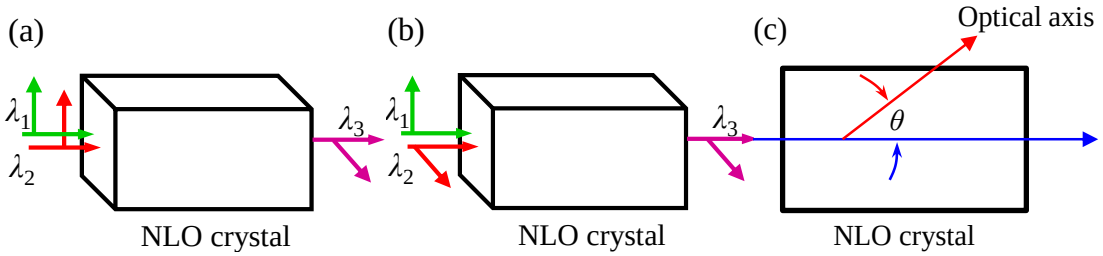

Fig. 1.3: *(a), (b) depict the Type-I, Type-II phase-matching with respect to the polarizations of the waves, here λ_1 λ_2 are the fundamental λ_3 is the harmonic or mixed wavelengths, and (c) the critical phase matching by angle tilting*

(i) **Type-I phase matching:** The polarization vectors of the interacting waves are parallel. The two incident beams (actually a single beam in the frequency doubling case) are oriented perpendicular to the optical axis of the crystal and the harmonic beam is polarized parallel to the optical axis of the crystal [Fig. 1.3(a)].

(ii) **Type-II phase matching:** The polarization vectors of the interacting waves are perpendicular [Fig. 1.3(b)].

A single linearly polarized fundamental beam may be divided into its *o* and *e* polarization components by orienting it at 45 degrees with respect to the X axis. The second harmonic beam will be polarized parallel to the optical axis of the crystal, 45 degrees from the incident beam. In *type II phase matching*, the two fundamental beams have different polarization directions; this can be appropriate when the birefringence is relatively strong (over compensating the dispersion in a *type I* scheme) and/or the phase velocity mismatch is small. The phase matching can be obtained by angle tilting as shown in the [Fig. 1.3(c)]. If the angle between optical axis and beam propagation (θ) isn't equal to 90^o or 0^o, we call it critical phase-matching (CPM). Otherwise, 90^o non-critical phase-matching (NCPM) is for $\theta=90^o$ and 0^o NCPM is for $\theta=0^o$. The phase matching can be obtained in the so called negative birefringent crystals ($n_e < n_o$) as depicted in Fig. 1.4(b) which shows the refractive index surfaces for a negative birefringent crystal. The value of n_o for both the fundamental and second harmonic i.e. n_o^{ω} and $n_o^{2\omega}$ are direction independent and the surfaces are circular; whereas for extraordinary ray n_e are elliptical and hence varies as a function of the angle with respect to the optic axis (θ).

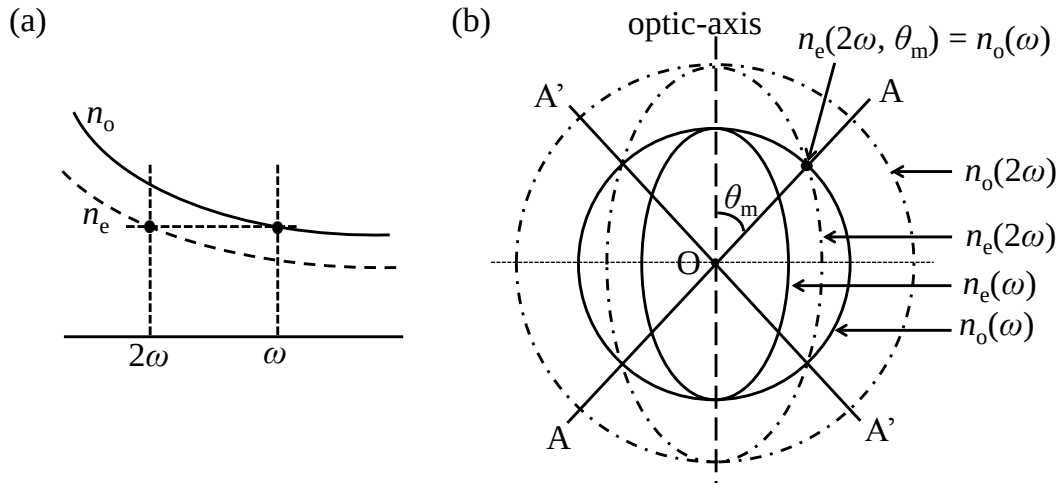

Fig. 1.4: (a) *The dispersion of refractive ordinary and extraordinary indices in uniaxial crystal and the phase matching, matching the index of -o at ω with that of -e at 2ω and* (b) *The indicatrix for a negative uniaxial crystal*

One can get the phase matching angle θ_m at the crossing of the refractive index surfaces of ellipse corresponding to n_o^{ω} and $n_e^{2\omega}$ i.e. where $n_o^{\omega} = n_e^{2\omega}(\theta) = n_e^{2\omega}(\theta_m)$. This phase matching condition is possible due to the birefringence of crystal having different refractive indices depending on the polarization of the wave, as shown in Fig. 1.4(a). So, from the refractive index surfaces one can get straight away the value of phase matching angle which can also be calculated. The refractive index of the harmonic is defined as a function of angle 'θ', given as,

$$\frac{1}{(n(\theta))^2} = \frac{\cos^2(\theta)}{(n_o^{\omega})^2} + \frac{\sin^2(\theta)}{(n_e^{\omega})^2} \tag{1.9}$$

with which the phase-matching angle 'θ' can be deduced for a value $n(\theta)$ at the harmonic wavelength to be equal to n_o. The phase matching condition is satisfied for all the directions at particular angle falling on the cone and the cone angle is termed as the phase matching angle 'θ_m'. This angle can be determined by the relation:

$$\sin^2\theta_m = \frac{(n_o^{(\omega)})^{-2} - (n_o^{(2\omega)})^{-2}}{(n_e^{(2\omega)})^{-2} - (n_o^{(2\omega)})^{-2}} \tag{1.10}$$

1.2.5.2 Beam *walk-off* and temperature tuning for 90° phase-matching

The indices of refraction of crystals not only dependent on the direction of *k*-vector and polarization of the transmitted waves but these also depend on the external influences that affect the lattice spacing of crystal in three dimensions,

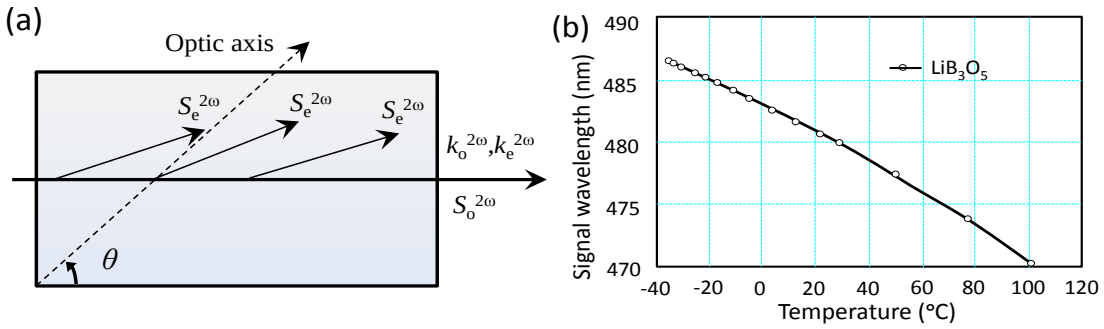

Fig. 1.5: (a) *The schematic presentation of Poynting walk-off process in the crystal, (b) a temperature tuning curve indicating the access of parametric generation in LiB3O5 crystal through the angle phase matching (Hanson & Dick, 1991)*

such as temperature. All the parameters n_e^{ω}, n_o^{ω}, $n_e^{2\omega}$ and $n_o^{2\omega}$ are temperature dependent and hence the phase-matching condition Δk can be achieved merely by changing the temperature of crystal. The beam walk-off gets included in phase-matching (*Type-I* & *Type-II*) process due to the participation of both *ordinary* and *extraordinary* rays. In collinear phase-matching all the wave vectors '*k*' point in same direction, but the ray directions or Poynting vectors '*S*' (directional energy flux density) are in different directions. The nonlinear generation usually involves narrow focused laser beams. Along the path of such a laser beam in the crystal medium, which follows the Poynting vector, the nonlinearly generated wave of orthogonal polarization will travel at different angle, this phenomenon is known as '*walk-off*' [Fig. 1.5(a)].

In the uniaxial crystals ($LiNbO_3$, KDP, ADP, proustite (Ag_3AsS_3) *etc.*) a highly desirable geometry results if the phase matching angle can be tuned, by eliminating the beam walk-off caused by double refraction. At different wavelengths the phase-matching conditions (Δk =0 & θ_m=90°) can be achieved by changing the temperature. The change in the refractive index with temperature at particular wavelength is required to be known and this shift in refractive index leads phase-matching condition achievement (Robert, 2003). The interacting beams are aligned such that they propagate along optical axis of the crystal and the phase mismatch is minimized by adjusting the crystal temperature, so that the phase velocities of the interacting beams are equal. The phase-matching criterion for second harmonic generation in –ve uniaxial crystal for *Type-I* process is given as;

$$(2\omega)\left(n_e^{2\omega}(T) + \frac{\partial n_e^{2\omega}}{\partial T}\Delta T \right) = 2\left(\omega\left(n_o^{\omega}(T) + \frac{\partial n_o^{\omega}}{\partial T}\Delta T \right) \right) \tag{1.11}$$

Here, T is the temperature and $\frac{\partial n_o^{\omega}}{\partial T}$, $\frac{\partial n_e^{2\omega}}{\partial T}$ are the changes in refractive indices for *ordinary* fundamental and *extraordinary* second harmonic waves, respectively, for the change in temperature of ΔT. This technique is termed as *noncritical* phase matching, because it relatively insensitive to the slight misalignment of the beams. The temperature tuning for the angle phase matching has been performed for LiB_3O_5 single crystal for the blue parametric generation Fig. 1.5(b), performed by Hanson & Dick (1991). The quadratic dependence of wavelength on temperature [$\lambda = 483.15 - 0.1068T - 0.000215T^2$] has been exhibited and the large *temperature tuning coefficient* (-0.11 nm/°C) has been obtained, which made temperature tuning possible over a large wavelength range.

1.2.5.3 Quasi phase matching by periodic poling

A special technique of significant importance is *quasi-phase matching*, where real phase matching does not occur, but high conversion efficiencies are nevertheless obtained in a crystal where the sign (or strength) of the nonlinearity varies periodically. This is because of the following fact that the typical dispersion values in the visible and near-IR of most crystals limits the coherence length to about 10 μm. Thus, the maximum output power will be very small. (If one could stack 10 μm thick sections of such a crystal in alternating fashion, it is possible to get around this limitation but such a structure would be prohibitively expensive if it could be fabricated at all). However, this is the concept of "*Periodically Poled*" non-linear crystals which could be well understood further by the following discussion.

For the birefringence phase-matching, some of the angles of propagation are not possible, therefore some of the nonlinear susceptibility tensor 'd_{ijk}' elements cannot be accessed. The underlying problem is that the phase of the second harmonic wave changes to the fundamental wave due to different light speeds in crystal owing to the dispersion. If we consider the direction of the incident wave is along the z-axis, then for z < coherence length, 'L_c', the harmonic power will build up from the fundamental wave to the maximum at L_c, corresponding to a phase shift π.

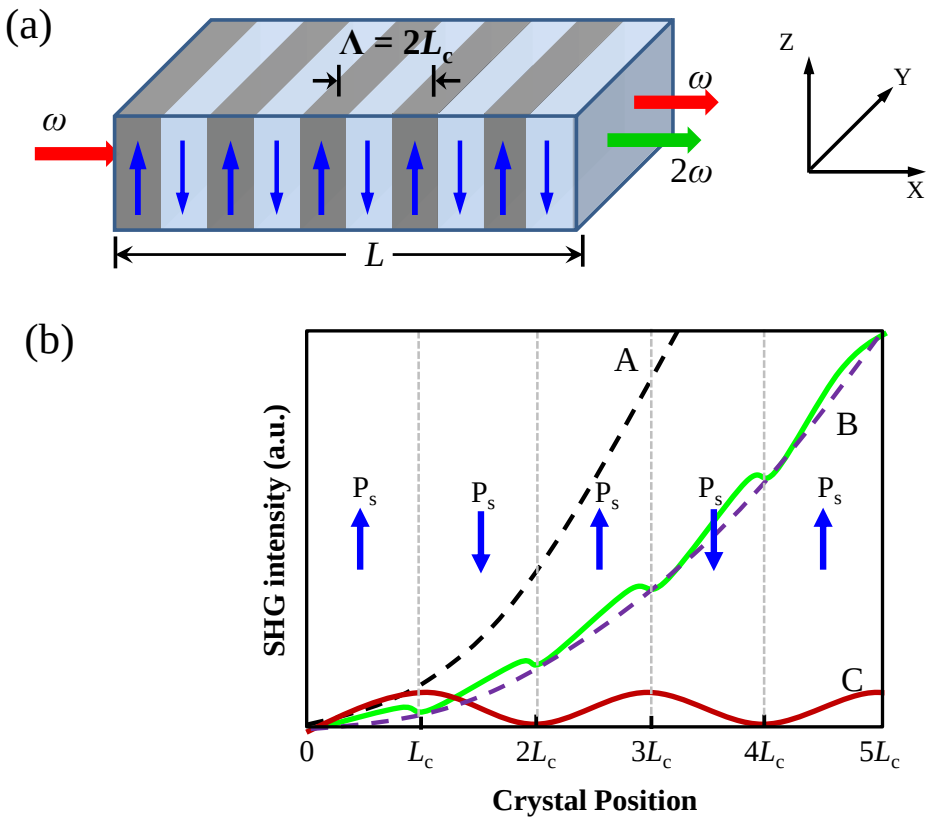

Fig. 1.6: (a) *The periodically poled domain structure for second harmonic generation and the Cartesian coordinate system (Bloembergen, 1965), (b) the A birefringence phase match, B QPM and C Phase mismatch processes (Manfred Wöhlecke et al., 2005)*

When $z > L_c$, the power couples back to the fundamental wave. However, for the monotonic growth of nonlinear intensity the sign of the polarization could be reversed by changing the sign of the effective nonlinear susceptibility tensor 'd_{eff}' at every coherence length, L_c, thus inducing a reverse phase shift, and allowing continuous constructive interference between the incident and harmonic waves which results in a buildup of the harmonic.

This structural artificially engineered phase matching condition is termed as the *quasi phase-matching* (QPM). Bloembergen and coworkers (Armstrong *et al.*, 1962; Bloembergen, 1965; Miller, 1964) have discussed to reverse the sign of the respective tensor element periodically after an appropriate crystal thickness and in ferroelectric materials, this could be done by antiparallel periodic poling of the crystal regions, ferroelectric domains (in micrometer 'μ' regime). This creates a sequence of nonlinear segments of opposite optical domain direction and thus cause in change of

polarization vector by π, by changing the sign of d_{ijk} coefficient in the successive domains of the order of 'L_c'. The QPM makes it possible to use the same polarization direction of all interacting waves and this often corresponds to using a stronger element of the nonlinear tensor. With this effect, the conversion efficiency can be significantly higher than for true phase matching. The QPM makes possible to avoid the spatial *walk-off* and suffice the large acceptance angle, it can also be adjusted in order to obtain a convenient temperature phase-matching (Fejer *et al.*, 1992; Myers *et al.*, 1995). It is therefore possible to operate the QPM at or near room temperature without resorting to critical phase matching or noncollinear phase matching.

The ferroelectric NLO crystals such as lithium niobate ($LiNbO_3$), $LiTaO_3$, potassium titanyl phosphate ($KTiOPO_4$), $BaTiO_3$, *etc.* are suitable for the fabrication of periodically reversed polarization domains, however, $LiNbO_3$ has been found to be technologically most suitable and the structures made from this are termed as periodically poled lithium niobate (PPLN). The Fig. 1.6(a) shows the schematic view of such a periodic poled QPM structure and this is referred as grating, here Λ is called the period of the grating. The red and green bold arrows indicate fundamental and SHG beams, respectively. The coordinate system at right side is to indicate the direction of propagating waves. To satisfy the phase matching condition for the process of nonlinear interaction, the momentum conservation condition is satisfied by the additional phase vector 'k_g' known as grating phase vector, as follows, $\Delta k = k^{2\omega} - 2k^{\omega} - k_g$. The grating phase vector k_g is given as $k_g = \frac{2\pi m}{\Lambda}$ and henceforth the period of grating 'Λ' has been described as $\Lambda = \frac{m\lambda_{\omega}}{2(n^{2\omega} - n^{\omega})} = 2mL_c$, here m is referred as the order of the quasi-phase-matched process and with m=1, $L_c = \frac{\lambda_{\omega}}{4(n^{2\omega} - n^{\omega})}$ is called first order quasi-phase-matching. The appropriate value of grating period can be chosen to satisfy compensate the phase mismatch. The intrinsic efficiency of QPM nonlinear process compared to that of birefringence phase-matching process is $4/m^2\pi^2$. Therefore first order (m = 1) QPM is preferred, shown in Fig. 1.6(b). Here, 'P_s' along with the upward and downward blue arrows indicate the upright and inverted spontaneous polarization of domains. The dashed parabolic black

curve A indicates the perfect birefringence phase matching over the entire length of crystal. The curve C indicates the condition of phase-mismatch with the coherence length of phase-match of L_c. The curve B represents the QPM of the first order, for a kind of periodically polarized structure [Fig. 1.6(a)].

Although the QPM is intrinsically less efficient, it overcomes some of the major problems which occur in birefringence phase-matching, including low effective nonlinear coefficient, inconvenient phase matching temperatures and angles, photorefractive damage and Poynting vector *walk-off*. In QPM the polarization and direction of input and output rays feasibly lies in the same plane, such as along one of the crystal axes. Due to this advantage in $LiNbO_3$, the d_{33} nonlinear coefficient can be used to increase the conversion efficiency by over 20 times to that possible with birefringence which uses the d_{31} coefficient. By suing PPLN in combination with common laser, the wide range of wavelengths in the entire visible and infrared can be processed for the nonlinear processed. The QPM is also possible to attain in the media in which the phase matching is otherwise impossible, for example in isotropic materials, or the materials with too high or too low birefringence at the required appropriate wavelength. A range of wavelengths in blue optical region is possible to generate by performing the temperature tuning.

1.3 THEORETICAL ASPECTS OF CRYSTAL GROWTH

Any crystal may be regarded as being built up by the continuing three dimensional transnational repetition of some basic structural pattern, which may comprise one or more atoms, molecule, or a complete assembly of molecules. Matter is more stable when its free energy attains to its minimum value. To come to a lowest energy state, the system has to release energy to its surroundings to compensate for the decrease in entropy by the ordering of atoms. This basic phenomenon is responsible for the crystal growth. Therefore, for the crystal growth to occur during which ordering of atoms or group of atoms takes place, the surroundings has to absorb the heat of crystallization produced during the process of crystallization by the reduction in entropy. However, the removal of heat of crystallization from the system should be well controlled to avoid multi-nucleation or rapid nucleation. For crystal

growth to occur, though the system should be away from the equilibrium state, its equilibrium should be maintained at near equilibrium and as near to a steady state process as possible. Methods along with basic theory used to grow single crystals along with their sub important categories depending upon the nature of the material are given below.

1.3.1 Theory of crystallization

Crystal growth is a controlled process of solidification of matter from its liquid or vapor state. This crystallization process in the first order phase transition involving two contacting phases, such as liquid–solid or vapor–solid, separated by an interface (Mullin *et al.*, 2001). In general, crystals grow in three different processes; (i) atoms and molecules are introduced into the crystal phase though the interface between crystal and growth medium, this is called kinetic process, (ii) atoms and molecules in the growth medium are supplied to the growth interface, or crystal surface, this is called volume diffusion process, and (iii) removal of latent heat generated at the growth interface during crystallization. The rate of crystal growth is determined by the rate at which the crystal pass through each of the above mentioned processes.

The spontaneous formation of crystalline nuclei in the interior of parent phase is called homogeneous nucleation. On the other hand, heterogeneous nucleation demands a pre-existing foreign crystalline substrate on which a new material can be deposited from the vapour, the melt or from solution (Pimpinelli & Villain, 1998; Santhanaraghavan & Ramasamy, 2000). For the growth of crystal some driving force is required, the conditions in any given system change according to the laws of thermodynamics in such a manner that the free energy in the whole system decrease. The crystallization process involves change in the *Gibbs free energy* ($G \equiv H - TS$) at the point of phase transition (Gibbs, 1878), is given by

$$\Delta G \equiv \Delta H - T.\Delta S \tag{1.12}$$

where, ΔG is the change in Gibbs free energy and S is the entropy of the system and T is the temperature. ΔH is the change is enthalpy, which is the *latent heat of transformation*, given by $\Delta H \equiv T\Delta S$. The behavior of *Gibbs free energy* with temperature for solid and liquid state is shown in Fig. 1.7(a), T_m is the

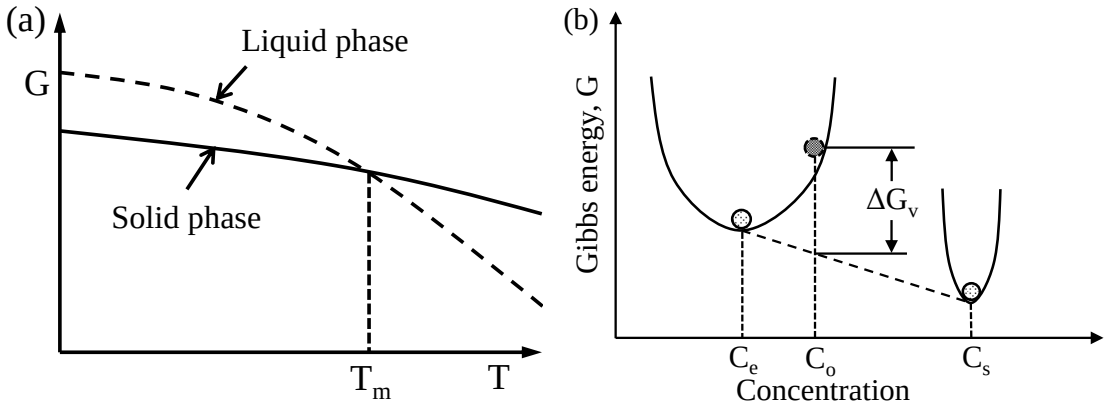

Fig. 1.7: *(a) behavior of the Gibbs free energy with temperature for melt and solid phases, (b) variation of Gibbs free energy with the concentration of solution during the solid phase formation*

melting temperature. At any temperature below T_m, the value of ΔG is given by $\Delta G = G_I(T) - G_{II}(T)$, where, $G_I(T)$ and $G_{II}(T)$ are the Gibbs free energy values for liquid and solid phase respectively. At the equilibrium state, Gibbs potentials of the two phases are equal, *i.e.* $\Delta G = 0$. Therefore, at the melting point T_m the value of ΔH becomes $T_m \Delta S$. Hence the driving force for crystallization from direct melt at a temperature T, using $\Delta H = T_m \Delta S$, is

$$\Delta G \equiv T_m.\Delta S - T.\Delta S = (T_m - T).\Delta S = \Delta T.\Delta S = \Delta H.\Delta T/T_m \qquad (1.13)$$

In case of the solutions the driving force for crystallization (Brice, 1967; Brice, 1969) is mainly the supersaturation. The solution with solute exceeding solubility or supersaturation, possesses a high Gibbs free energy, the overall energy of the system would be reduced by segregating solute from solution. Figure 1.7(b) shows the reduction of the overall Gibbs free energy of the supersaturated solution by forming a solid phase and maintaining an equilibrium concentration in solution. This reduction in Gibbs free energy is the driving force for nucleation and growth, the change in Gibbs free energy per unit volume, ΔG_v, is dependent on the concentration of solute and expressed as follows;

$$\Delta G_v = aRT \ln\left(\frac{C}{C_e}\right) = aRT \ln\left(1 + \frac{\Delta C}{C_e}\right) \quad \text{or} \quad \Delta G_v \approx aRT \ln\left(\frac{\Delta C}{C_e}\right) \qquad (1.14)$$

where, C is the actual concentration of solute, C_e is the equilibrium concentration or solubility, ΔC ($= C - C_e$) is called supersaturation, a is a constant and R is the gas constant. Without supersaturation (i.e., $\Delta C = 0$), ΔG_v is zero, and no nucleation will occur and when $C > C_e$ the nucleation will occur spontaneously. Various studies have

been carried out regarding the dependence of growth kinetics on the supersaturation of solutions (Bennema, 1967, 1969). The crystal growth mainly consists of two steps, viz. nucleation and subsequent growth of the nucleus in the form of bulk crystal, discussed in the next section.

1.3.2 Nucleation

Nucleation is the process of conglomeration of atoms or molecules to form the first sub-microscopic speck or nucleus of crystalline phase, known as "embryos", with new surfaces which may subsequently grow to produce a tangible crystal. The theory for the formation of nucleus was given by Volmer and Weber, with the consideration of total free energy for a group of atoms/molecules in the nucleus (Volmer & Weber, 1925). The surface free energy associated with the crystal-liquid interface increase as the nucleus grows. Thus formation of the new phase is energetically at higher free-energy state than the existing mother phase, therefore the new crystalline phase has tendency to dissolve back into the initial mother phase. Formation of nuclei smaller than a critical size causes an initial increase in the free energy due to the need to create surface(s) and, therefore, is not thermodynamically favorable. The probability that the nuclei will grow to form stable nucleus of critical dimension depends on the change in free energy associated with its formation. As the nuclei grow larger, the free energy reaches a maximum and becomes negative, leaving the stable nuclei. The nucleation is mainly of two types: (i) Primary nucleation, the nucleation without presence of any crystalline matter, in this the potential barrier to overcome for new phase to crystallize is a function of interfacial energy between the crystal and the mother phase and the thermodynamic driving force. (ii) Secondary nucleation, this is induced by the already present crystallites. Primary nucleation generally takes place comparatively at higher supersaturation and is further subdivided into homogeneous/spontaneous in clear solution and heterogeneous in the solutions containing dust, impurities or solid surfaces which influence the potential barrier. Formation of a new stable phase 'embryo' comprise of the free energy associated with its volume and surfaces. The behavior of associated energies with size of nuclei is shown in Fig. 1.8(a). The total Gibb's free energy change, ΔG of the embryo between the two phases associated with nucleation process is given as,

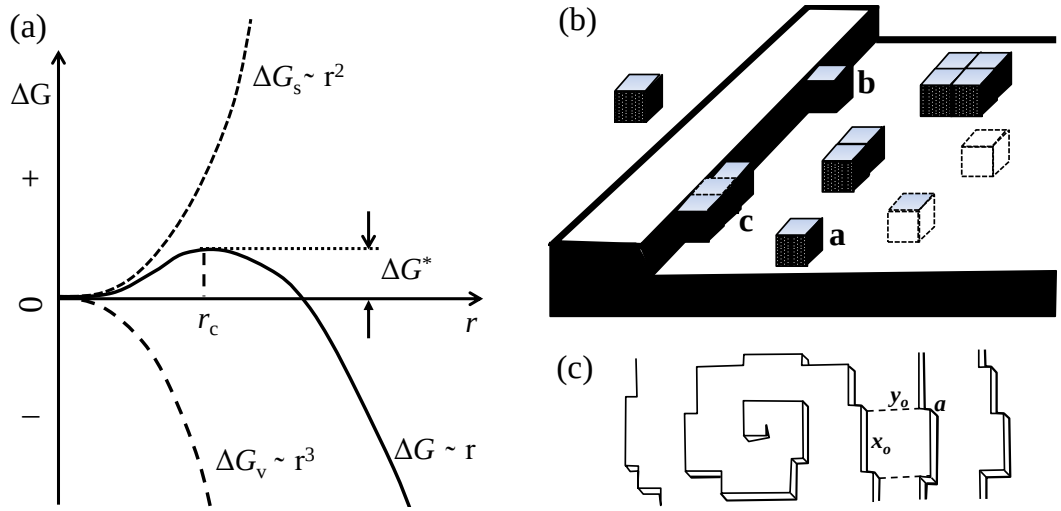

Fig. 1.8: *(a) The plots of Gibbs free energy change with the size of nucleus, indicating the behavior of ΔG_s, ΔG_v, and ΔG , (b) two dimensional layer growth, and (c) screw dislocation growth process*

$$\Delta G = \Delta G_s + \Delta G_v \tag{1.15}$$

where, ΔG_s is the surface free energy and ΔG_v is the volume free energy of the system decreased for each unit volume. If the σ is the increased interfacial energy per unit area of the formed solid-liquid interface, then, the Gibbs free energy change associated with the formation of a spherical nucleus of radius r is given by

$$\Delta G = 4\pi r^2 \sigma + (4/3)\pi r^3 \Delta G_v \tag{1.16}$$

In Fig. 1.8(a) the solid line graph for ΔG is the contribution of both the surface and volume free energy changes. The surface energy increases with r^2 and the volume free energy decreases with r^3. The net free energy change first increases with radius of nucleus, attains a maximum and then decreases for the further increase in the size of nucleus. The size of the nucleus corresponding to the maximum total free energy is called as 'critical nucleus', and this is the smallest sized embryo which can grow further effecting the reduction in free energy of the system. On the other hand if the size of the formed nucleus is below the critical dimension, no further growth of nucleus is possible and it will re-dissociate into the mother phase. At the critical/stable size of the nucleus, r_c,

$$d\Delta G / dr = 0 \tag{1.17}$$

with this condition, the solutions of equation (1) for r_c and ΔG^*, are given as

$$r_c = -2\sigma / \Delta G_v \quad \text{and} \quad \Delta G^* = 16\pi\sigma^3 / (3\Delta G_v^2) \tag{1.18}$$

Here, the critical radius condition is evaluated with consideration of spherical nucleus if the nucleus is considered non-spherical then the numerical factor 2 in the numerator will be different. ΔG^* is the energy barrier that a nucleation must overcome, shown in the graph Fig. 1.8(a) (Mullin, 2001). These expressions for critical radius and critical free energy change are based on a supersaturated solution; however, all the concepts can be generalized for a supersaturated vapor and a supercooled vapor or liquid. Free-energy barriers for homogeneous nucleation are higher than those for heterogeneous nucleation, and hence the level of superstauration or supercooling required is higher.

1.3.3 Subsequent growth of nuclei

Once the nuclei has crossed the critical-size barrier, the further growth of it into crystal requires the supply of growth species atoms/molecules to the growth surface through interface, and removal of heat, released during crystallization (latent heat of crystallization), away from the site. The rate of growth depends on how rapidly the latent heat of crystallization can be removed from the growing crystal surface. Growth process consists of several consecutive steps of mass transfer, by convection or diffusion, of solute species through the interface from solution to crystal surface, adsorption of solute and integration of the solute species (i.e. atoms or molecules) into the growth sites. Various theories have been developed to elucidate the mechanism and rate of crystal growth (Volmer, 1939; Kossel, 1927; Stranski, 1928; Bethe, 1935). Volmer has proposed the layer by layer growth of crystal faces and provided the concept the atomic picture of crystal growth and defined the solid liquid interfaces. Kossel & Stranski defined the kink, step, and flat sites, at which the growing species adsorbed and integrated into a crystal. The two-dimensional layer growth and screw dislocation theory are the main theories to describe the growth of the single crystals.

1.3.3.1 Two dimensional layer growth theory

Volmer has suggested, the growing units arriving at the crystal surface do not immediately enter to the crystal lattice, but lose their degree of freedom and become

free to move over the surface. Such a typical unit is indicated by (unit **a**) in the schematic of Fig. 1.8(b), it is loosely attached with the surface It gets tightly attached to the surface by losing one more degree of freedom, viz. as unit **b**. Finally it loses all degrees of freedom by settling into some kink and get crystallized, unit **c**. This process continues till the whole layer (plane) is completed. In two-dimensional nucleation theories, for low values of the supersaturation a meager or no growth is expected. The theory given by Burton *et al.*, (1952) suggested that for measureable growth rate the supersaturation should be at least 25 – 50%. However, Volmer & Schultze, (1931) have found that the crystals do grow at the observable rates even at the supersaturation of 1%, this could not be explained by two-dimension nucleation theory.

1.3.3.2 Screw dislocation theory

To explain the shortcoming of above theory at low supersaturation, Frank (1949) has suggested the presence of imperfection in growing crystal. According to the theory given by Burton, Cabrera and Frank (BCF), the screw dislocations on the face of crystal produce the ledges of height of Berger's vector and the growing species attach to these ledges in the form spirals, and the growth proceeds by widening of these spirals as shown in Fig. 1.8(c). The characteristics of the surface structure for growth model are kink distance (x_o) step distance (y_o), and the step height (a), as shown in the figure. Verma (1951 & 1953), and Griffin (1950), have experimentally verified the presence of screw dislocation as the growth sites.

1.4 SINGLE CRYSTAL GROWTH METHODS

The single crystals of the materials can be grown from the solid, liquid or vapor phase according to the feasibility materials (Laudise, 1970; Brice, 1965; Jackson, 1958; Mullin, 1965). Different growth methods have been opted, depending on the above individual process. The classification of growth methods is given in brief as follows.

1.5.5 Melt growth

The melt growth has great technical as well economic importance because in this the bulk single crystals can be efficiently grown with unlimited size at higher growth rates. This is the process of crystallization by fusion and re-solidification of the material. Solidification of the melt provides a simple method for the growth of the crystals which melt congruently and have reasonably low melting point. In this technique apart from the contamination from crucible material and surrounding atmosphere, no impurities are introduced in the growth process and the rate of growth is normally much higher than possibly other methods.

With the suitability of different materials, there is a variety of melt-growth techniques. Some of the main techniques are enlisted here:

(i) Czochralski or pulling Method (Czochralski, 1918)
(ii) Bridgman Method (Bridgman, 1924; Stockbarger, 1936)
(iii) Verneuil Technique (Verneuil, 1890, 1902-1904)
(iv) Kyropoulos Method (Kyropoulos, 1926)
(v) Edge-defined, Film Fed Growth (LaBelle Jr., 1971)
(vi) Zone Melting/ Float Zone Technique (Pfann, 1952; Keck & Golay, 1953)
(vii) Heat Exchanger Method
(viii) Skull Melting

In the Czochralski method the growing crystal is pulled-out from the crucible containing the melt, whereas in case of Kyropoulous method pulling of the crystal is not performed but the crystal grow onto a seed inside the crucible. In Bridgman technique the progressive crystallization of melt is performed, loaded in vertical or horizontal ampoule.

In the present thesis work, for the growth of bulk single crystals of pure, Zn- and Fe-doped $LiNbO_3$ and pure and liquid crystal induced Benzophenone the Czochralski growth technique has been used. The description about the Czochralski technique and experimentation is described in detail, in Chapter-2.

1.4.2 Solution growth

Materials, which melt incongruently or decompose before melting or undergo a phase transformation between room temperature and the melting point, are generally grown by the solution method (Bordui, 1987). In this method the crystal grow with their facets freely in the natural habit, which advantages in the identification of crystallographic axes. The trapping/incorporation of solvent molecules inside the crystals is disadvantageous, which may be avoided by choosing the solvent carefully. The different aspects to be considered for solution growth process are: (i) the solution chemistry (how efficiently the solvent ions break the bonds of solute molecules), (ii) solubility *vs.* temperature curve, (iii) metastable zone limit (to maximize growth rate), *etc*. There are other methods for the solution growth, such as high temperature solution growth called flux growth technique. The oxides such as yttrium iron garnet (YIG), lead zirconate titanate (PZT) *etc*., are mostly grown by the flux method. Materials having high MPs are dissolved in a suitable solvent (flux) at high temperatures. Growth from the flux is generally achieved by decreasing the temperature of the saturated solution very slowly to achieve super saturation. As the temperature is decreased, supersaturation increases and the nucleation takes place and slowly attains bigger size. This method very slow and purity of the crystal grown by this method is not good, the stoichiometry control is also very difficult. Inclusions of flux in the grown crystals are a general problem. Due to these limitations it is not the preferred technique to grow single crystals with large dimensions.

As per the suitability of growth of bulk crystals of particular material the different methods have been developed/ invented and the major solution methods are enlisted here:

(i) Slow-cooling method
(ii) Slow evaporation solution method
(iii) Temperature gradient method (Yongzong, 1986)
(iv) Seed rotation method (Watanabe *et al.*, 1981)
(v) Sankaranarayanan-Ramasamy method (Sankaranarayanan & Ramasamy, 2005)

The newly invented Sankaranarayana-Ramasamy (SR) method advantages to grow the crystals in desired direction/ shape of unlimited size with ~100% solute to crystal conversion efficiency.

For the growth of single crystals of pure, urea and chromium doped tris(thiourea)zinc sulphate (ZTS), the slow evaporation technique (SEST) has been employed, therefore, it has been briefly described in the next chapter.

1.4.3 Vapor phase growth

Vapor growth techniques can be adopted for the growth of materials which lack a suitable solvent and sublime before melting (Faktor & Garrett, 1974). Vapour growth methods have been employed to produce bulk crystals and to prepare thin layers on crystals with a high degree of purity. A variety of materials are available in vapour phase with controlled level of impurities and device quality crystals, can be grown. The vapour phase growth is very slow like the solution growth. Therefore, this is chosen for the growth of bulk crystals only when it is not possible to grow the crystals by other techniques. However, to grow thin layers of materials such as Si, II-VI and III-V compound semiconductors, this method is widely employed, especially for epitaxial growth (Kaldis & Schieber, 1971). These are further devided into the following sub-techniques.

(i) Metal-oxide chemical vapor deposition (MOCVD)

(ii) Molecular beam epitaxy (MBE)

1.5 IMPERFECTIONS/ DEFECTS IN SINGLE CRYSTALS

Due to different thermal gradients at different spatial locations in the growing crystal, even the same crystal may contain defects with different densities and sizes. These defects strongly affect the physical properties of single crystals. The major defects in single crystals are categorized as; (1) Grain boundaries, (ii) Low angle or subgrain boundaries, (iii) Dislocations, (iv) Stacking faults, and (v) point defects and their aggregates.

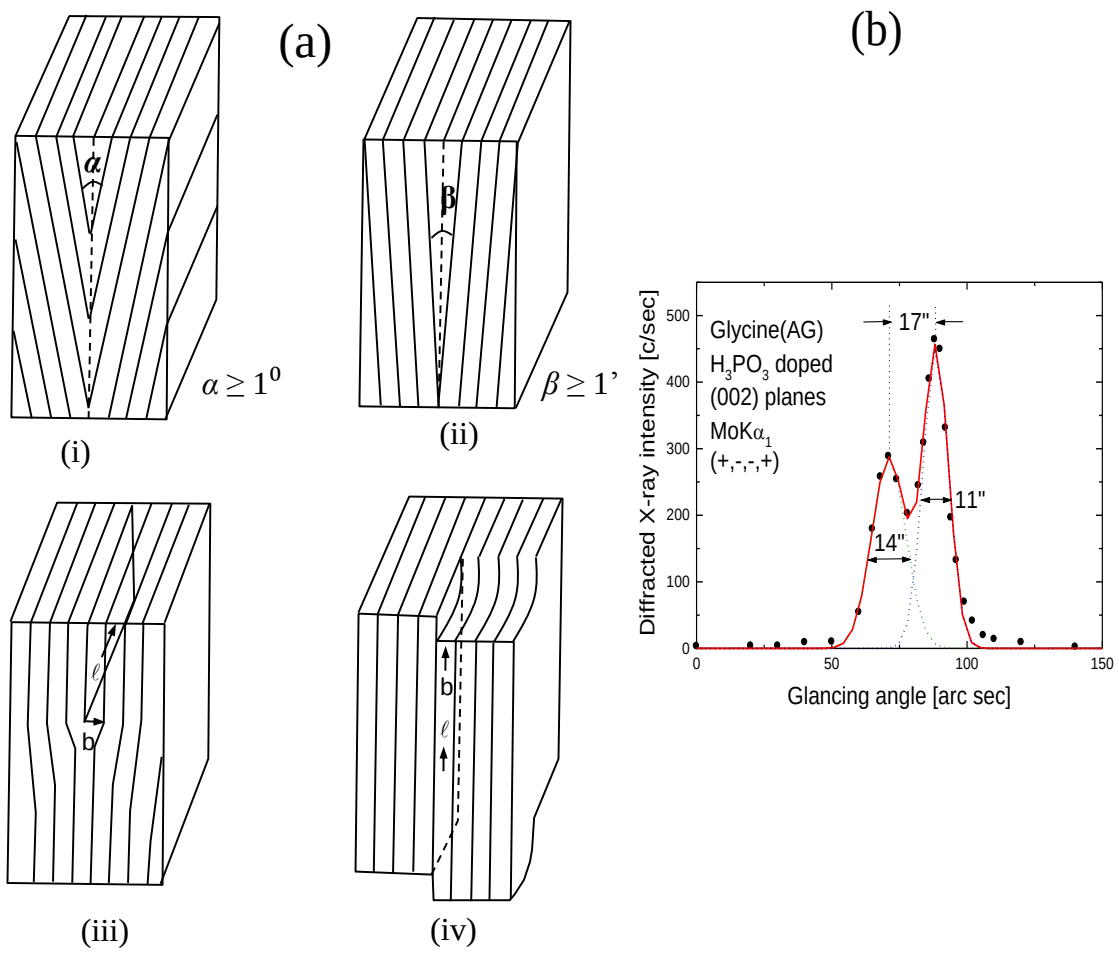

Fig. 1.9: *Line schematic of crystal defects; (a): (i) a grain boundary, (ii) a subgrain boundary, (iii) an edge dislocation and (iv) a screw dislocation, and (b) the rocking curve of a crystal showing a very low angle grain boundary (detectable only by high resolution transmission electron microscopy or high resolution X-ray diffractometry)*

1.5.5 Grain boundaries

A grain boundary is an imperfection which separates two small crystallites (grains) of a crystal, crystallographically misoriented by about a minute of arc more with each other (Chaudhary & Mathews, 1972; Lal, 1989). Grain boundaries have a strong influence on mechanical, physical and electronic properties (Bhagavannarayana, 1994).

1.5.2 Low angle or subgrain boundaries

The subgrain boundaries or the low grain boundaries separate regions of the crystals which are crystallographically misoriented with respect to each other by a few minutes of arc. Schematically these boundaries are shown in Fig. 1.9(a). These

boundaries can be understood in terms of an array of closely spaced dislocations. Prominent among these are tilt boundaries, twist boundaries and mixed type boundaries (Lal & Kumar, 1978). Figure 1.9(b) shows the rocking curve recorded by a high resolution multicrystal X-ray diffractometer, for (002) diffraction planes phosphoric acid doped α-glycine single crystal The rocking curve consists of an additional peak along with the main peak, depicting the presence of a *very low angle grain boundary* (FWHM < 1'). Such very low angle grain boundaries are detectable by high resolution transmission electron microscope or high resolution X-ray diffractometer, used in the present work.

1.5.3 Dislocations

The dislocation is a line imperfection which is the boundary between a region of an internal surface over which the slip has occurred and another region over which no slip taken place (Polanyi, 1934; Orowan, 1934; Taylor, 1934). A line vector **n** (vector of unit length parallel to the life of dislocation at any point) and a Burgers vector **b** (a translation vector indicates the direction and extent of lattice shift with respect to the lattice below the slip plane) (Hull, 1965) characterize the dislocation. Dislocations are of two basic type; edge dislocation, the Burgers vector is perpendicular to the line vector (**b** $\perp$ **n**) and (b) screw dislocation, the Burgers vector is parallel to the line vector (**b** $\parallel$ **n**) and are shown in Fig. 1.9(a).

1.5.4 Stacking faults

The stacking faults is an error in the stacking of atomic lattice planes which results from the stacking of one atomic plane on another out of sequence, so that the lattice on both sides of the fault have same orientation but are translated less than a translation vector with respect to another. This can be visualized to form due to splitting of a dislocation into two partial dislocations. In close packed structures such as **hcp** and **fcc** the stacking of layers perpendicular to C-direction have large number of possibilities. This is because the energy difference between the various possible stacking sequences is very small. This leads to a large number of possible stacking sequences and hence crystallographic structures. This phenomenon is known as polytypism (Verma & Krishna, 1969).

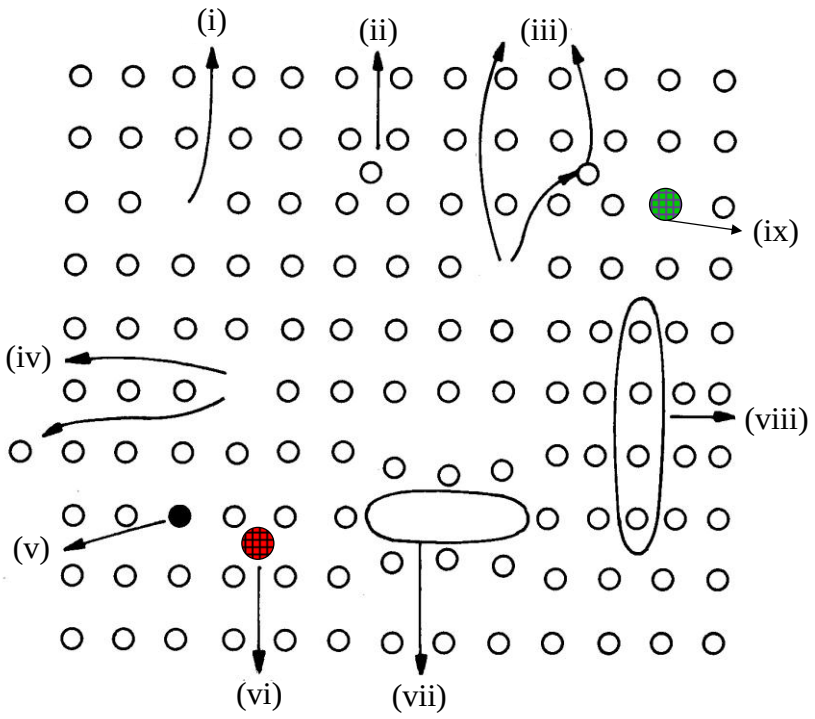

Fig. 1.10: *The point defects and their agglomerates: (i) vacancy, (ii) self-interstitial, (iii) Frenkel defect, (iv) Schottky defect, (v) sustitutional impurity, (vi) impurity atom at interstitial site, (vii) vacancy cluster, (viii) interstitial cluster, and (ix) an antisitic defect*

1.5.5 Point defects and their aggregates

The common point defects in single crystals are: (i) vacancies, (ii) interstitials (self interstitials) and (iii) foreign atoms: dopants or unavoidable impurities, and shown in the schematic of Fig. 1.10. The absence of an atom from a normally occupied site is known as *vacancy* and an atom displaced from the regular positions and lying in between the regular lattice sites or interstices is known as a self *interstitial*. In the ionic crystals due to the thermal vibrations when an atom leaves its site and occupies the interstitial position, the resultant vacancy and interstitial atom are known as *Frenkel defects* (Frenkel, 1926). In the event when an atoms leaves its lattice site (creating a vacancy) and moves to the external surface of the crystal, the vacancy so created is known as *Schottky defect* (Wagner & Scottky, 1930). In ionic crystals thermally created cation or inion vacancy is accompanied by creation of vacancy of opposite charge, hence generated anion-cation pair is also known as *Schottky defects* (Wagner & Scottky, 1930). A foreign atom which occupies the regular site of crystal is known as *substitutional impurity atom* and when it intersite

between matrix atoms, is called *interstitial impurity atom*. In the certain ionic crystals such as $LiNbO_3$ due to composition variance few of the atoms occupy the lattice sites of other atoms and result in *antisitic* defects. At the equilibrium state of crystal the number of vacancy defects present in the crystal lattice can be given by the relation;

$$N_v = N_0 \exp(-E_{av} / kT) \tag{1.19}$$

where, N_0 is the number of lattice sites/cm^3, E_{av} is the activation energy required to create a vacancy defect, k is the Baoltzmann constant and T is the absolute temperature. The value of E_{av} for silicon is ~ 2.6 eV. The equilibrium concentration of self-interstitials, N_i, is given by the relation;

$$N_i = N_0 \exp(-E_{ai} / kT) \tag{1.20}$$

where, E_{av} is the activation energy required to create a self-interstitial defect. The value of E_{ai} for silicon is ~4.5 eV. Due to the formation of energy for vacancies is very low therefore in general pure single crystals prominently contain the vacancy defects.

At high temperature the concentration of point defects is very high and during cooling process the faction of interstitials and vacancies trap in the lattice and defects, excess of the equilibrium, condense or segregate into aggregates (agglomerates) (de Kock, 1977). This happens to reduce the total energy of the system (crystal + defects). The agglomerates can take shape of disc, dislocation loop, spherical, needle, swirls, *etc.* (Bhagavannarayana, 1994).

Generally the structural defects in crystals are harmful and influence the efficiency of the devices based on these crystals. However, for certain applications the defects are being created in the crystals by using suitable dopants or physical processes, *e.g.* Tl doping in NaI (Tl:NaI), Nd doping in yttrium aluminium garnet (Nd:YAG), *etc.* Therefore, it is extremely essential to evaluate the crystalline perfection of grown single crystals before subjected to the device applications. In the present thesis, for defects analysis crystalline perfection assessment of the grown single crystals the multicrystal high-resolution X-ray diffractometer (HRXRD) has been employed. The details about the diffractometer are given in Chapter-3.